# Time-resolved Fourier transform spectroscopy of pulsed discharge products

**ARTICLE** *in* CHEMICAL PHYSICS LETTERS · FEBRUARY 2003

Impact Factor: 1.9 · DOI: 10.1016/S0009-2614(02)02017-1



**5 AUTHORS**, INCLUDING:

Oleg I. Baskakov
V. N. Karazin Kharkiv National University
**47** PUBLICATIONS **263** CITATIONS

Available online at www.sciencedirect.com
SCIENCE DIRECT®
Chemical Physics Letters 369 (2003) 293–298
CHEMICAL PHYSICS LETTERS
www.elsevier.com/locate/cplett

# Time-resolved Fourier transform spectroscopy of pulsed discharge products

Kentarou Kawaguchi *, Oleg Baskakov [1], Yukio Hosaki, Yoichi Hama, Chinatsu Kugimiya [2]

*Department of Chemistry, Faculty of Science, Okayama University, Tsushima-naka 3-1-1, Okayama 700-8530, Japan*

Received 20 September 2002; in final form 25 November 2002

**Abstract**

A time-resolved Fourier transform spectroscopic method has been developed with a microcontroller SX and a high-resolution Bruker IFS 120 HR. During one cycle of the He–Ne laser fringe, 30 data points are recorded with a preset time interval of 2 or 3 μs. The present system is applicable for any commercial continuously scanning interferometer. This method is applied to a pulsed discharge in an Ar and $H_2$ mixture to observe time profiles of Ar, ArH, and $ArH^+$ emission spectra. Pulsed afterglow was found to be an efficient source for the ArH radical. ArH and $ArH^+$ showed different time profiles, depending on the production mechanism.


## 1. Introduction

Time-resolved spectroscopy is of interest in various fields of chemical reaction studies. Most of the time-resolved Fourier transform spectroscopy (FTS) studies have been carried out using step scan type spectrometers with which it is easy to couple a pulsed discharge, pulsed laser and/or pulsed valve experiments. Durry and Guelachvili [1] reported time-resolved high resolution spectra of the $B^3\Pi_g$–$A^3\Sigma_u^+$ band of the nitrogen molecule produced by a microwave discharge. Several other instrumental advances have since been reported [2,3] with the Connes-type interferometer of CNRS Orsay. The frequency resolution is limited in commercial step scan type spectrometers, as seen in the study of highly vibrationally excited molecules reported by Letendre et al. [4].

Use of a continuously scanning spectrometer for time-resolved spectroscopy has been attempted by several groups. The idea is more or less similar to the first report of Murphy et al. [5]. However, the implementation is different depending on the rapidly evolving computer systems and electronics. Berg and Sloan [6] developed a compact stand

* Corresponding author. Fax: +81-86-251-7853.
*E-mail address:* okakent@cc.okayama-u.ac.jp (K. Kawaguchi).
[1] Visiting professor from Faculty of Quantum Radiophysics, Kharkov National University, Svobody Sq. 4, 61077 Kharkov, Ukraine.
[2] Permanent address: Osaka Minato High school, Namiyoke 2-3-1, Osaka 552-0001, Japan.

0009-2614/03/$ - see front matter 
doi:10.1016/S0009-2614(02)02017-1

alone data acquisition system for submicrosecond time resolved FTS. Nakanaga et al. [7] applied a pulse discharge system to a continuously scanning interferometer without any modification to the software of the system. Weidner and Peale [8,9] developed a low-cost system for time-resolved FTS by using an event-locked technique, compensating the mirror speed variations.

In the present study, we have developed a time-resolved FTS by using a programmable microcontroller SX which operates with a 50 MHz clock. This is a new system which uses recently available electronic facilities and is applicable to any continuously scanning FTS and has advantage in flexibility with easy set-up. The system is applied for emission measurements from a pulsed discharge in a mixture of Ar and $H_2$ to measure the time profiles of Ar, ArH, and $ArH^+$ emission lines.

## 2. Experimental

The schematics of the experimental setup used with a Bruker IFS 120HR FT spectrometer in the present study is shown in Fig. 1. The present experiment was done in emission from a discharge. The discharge was induced in a water-cooled glass cell using a high-voltage power supply and a transistor switch HTS 81 (Behlke electronic GmbH, Frankfurt, Germany). The inner diameter of the cell was 15 mm and the length was 250 mm. Radiation from the discharge plasma was focused on the iris of the interferometer by a $CaF_2$ lens with

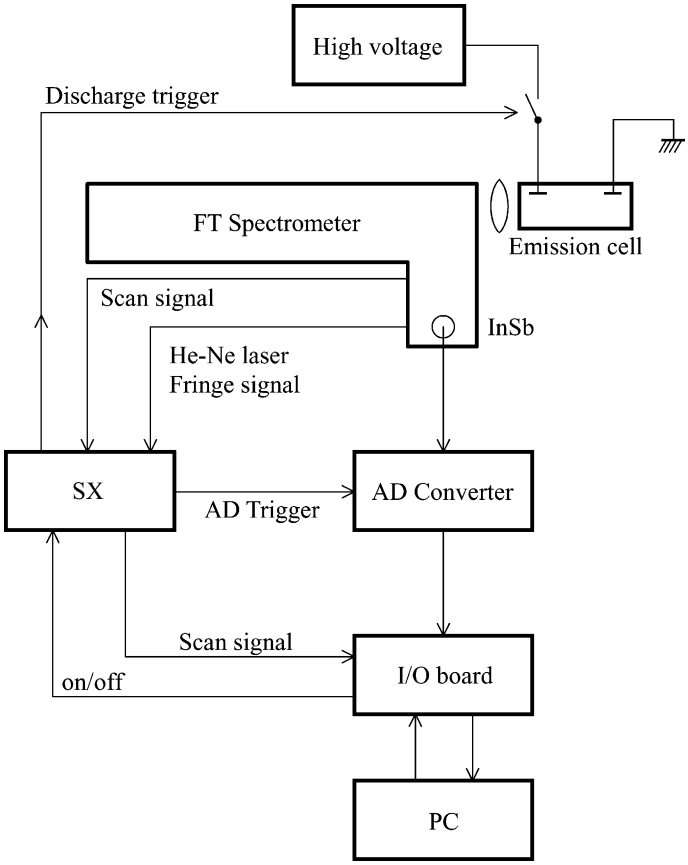


Fig. 1. Block diagram of the time-resolved FTS. SX is a microcontroller. The analog to digital (AD) converter is ADC 4322 (16 bits, 2 MHz). Input board is PCI-2172C. PC is a personal computer with Celeron 800 MHz microprocessor.

a focal length of 50 mm. Radiation passing through the interferometer was detected by an InSb detector and fed into an analog to digital converter (ADC 4322: Analogic, USA) and the data were processed in a personal computer (PC). The 16 bit AD converter has a speed of 2 MHz. The digitized data were transferred to a digital input board PCI-2172C (Interface, Tokyo, Japan) through a PCI bus.

The SX (Parallax, USA) consists of a single chip computer which operates with a 50 MHz clock independently. Each process in the SX is programmed by assembly language. The role of the SX in our experiment was to produce a discharge trigger signal and AD trigger signals synchronously with the He–Ne laser fringe signals from the spectrometer, as shown in Fig. 2. It also controls the data transfer to the PC. Waveforms produced by the SX are also available from usual logic circuits. However, the usage of the SX allows us to change parameters easily through programming. Computer programs for data acquisition and processing and display were written in C++ language. A series of data corresponding to each AD trigger are stored and Fourier transformed. Thirty spectra at a preset time interval are obtained in each measurement.

The time resolution is 1 μs which is limited by the detector amplifier. Measurements were done in the region 1800–4000 $cm^{-1}$ with an optical filter, and the wavenumber resolution was 0.07 $cm^{-1}$. The observation time for the accumulation of 64 scans was 36 min under the above condition.

## 3. Observed spectra

Fig. 3 shows a part of the observed emission spectrum from a discharge in a mixture of Ar and $H_2$, where the partial pressures are 465(3.5) and 2.0(0.015) Pa(Torr), respectively. The discharge was initiated at time zero and turned off at 20 μs, at which stage we monitored the discharge current by using a register inserted at the cathode site and confirmed that the current became zero after 1–2 μs. The peak current was 0.5 A. For AD triggers, we used 3 μs for the zero offset and interval values, that is, AD conversion occurs every 3 μs from the start of the pulsed discharge and 30 pulses cover 90 μs. Lines with strong intensities in Fig. 3 are due to Ar atomic emission lines and are observed as two intense peaks. It is noted that the second peak appears after the discharge is off. The relative intensity of the second peak is largely dependent on the $H_2$ pressure. It is due to the afterglow plasma which exists for a short duration after turning off the discharge. When pure argon is used in the discharge, the second peak becomes weaker. It becomes stronger when a small amount of $H_2$ is added and the strongest intensity was obtained at

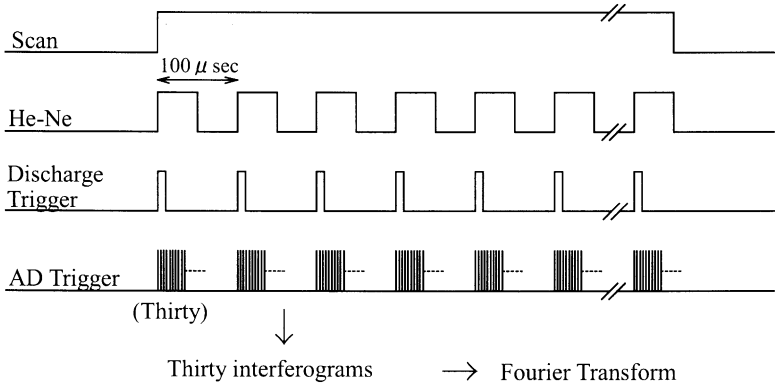


Fig. 2. Timing diagram for time-resolved FTS. The scan and He–Ne fringe signals are supplied from the Bruker 120 HR spectrometer. The time interval of 100 μs can be set by changing the velocity of the scanner, depending on the time profile of the system under study. The discharge trigger with the desired width is produced by SX programming. Thirty AD trigger signals are also supplied from SX by setting an offset time and interval by using the He–Ne laser fringe signal as a time standard. In one scan, 30 interferograms are obtained, and the Fourier transforms give 30 spectra at preset time intervals.

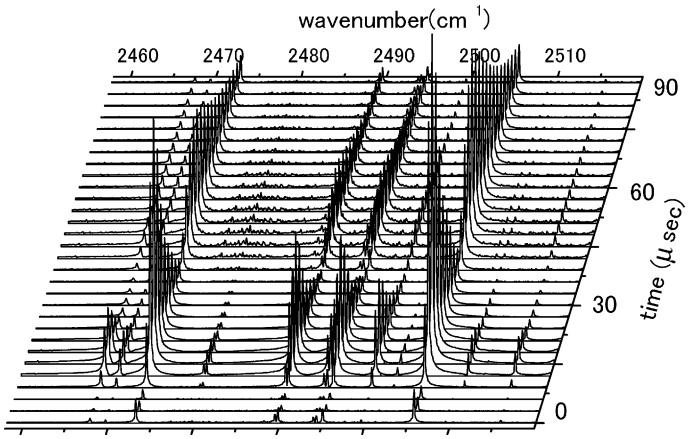


Fig. 3. A part of the observed emission spectrum from a discharge in an Ar 465 Pa and $H_2$ 2.0 Pa mixture. The discharge was applied in the interval 0–20 μs with a peak current of 0.5 A. The strong peaks are due to Ar atomic lines. Many weak lines seen around the second peak of Ar appear to be due to ArH but have not been assigned.

2.0(0.015) Pa(Torr) of $H_2$ (low $H_2$ pressure conditions: Figs. 3 and 4). Further addition of $H_2$ decreases the intensity of the second peak, as shown later.

Time profiles of the Ar atomic line, $6s[1\ 1/2]_2$–$5p[2\ 1/2]_3$ at 2740.323 $cm^{-1}$ and ArH line $^2\Pi(5p)$–$^2\Sigma^+(6s)$, R(6.5) at 3700.774 $cm^{-1}$ are shown in Fig. 4. The $^2\Pi(5p)$–$^2\Sigma^+(6s)$ band of ArD is analyzed by Dabrowski et al. [10]. The rotational assignment of the same band of ArH was carried out in the present study. It is noted that the ArH radical has one peak which coincides with the second peak of the Ar atomic line. The ArH line does not appear during the actual discharge, but it produced efficiently in the afterglow. The time profile of the $ArH^+$ ion signal was different from those of Ar and ArH, that is, only one peak appeared around 30 μs and the intensity gradually decreased until 80 μs.

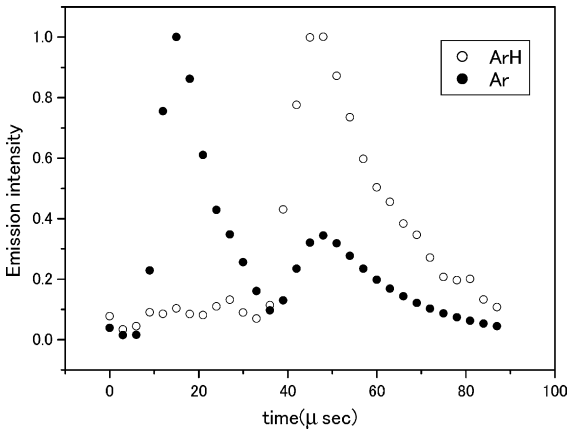


Fig. 4. Observed time profiles of emission intensities (arbitrary unit) of Ar $6s[1\ 1/2]_2$–$5p[2\ 1/2]_3$ transition at 2740.323 $cm^{-1}$ and ArH 5p–6s, R(6.5) transition at 3700.774 $cm^{-1}$ with the same discharge conditions as in Fig. 3. Data are taken every 3 μs. The magnitude of the error is 0.07 for ArH and 0.005 for Ar.

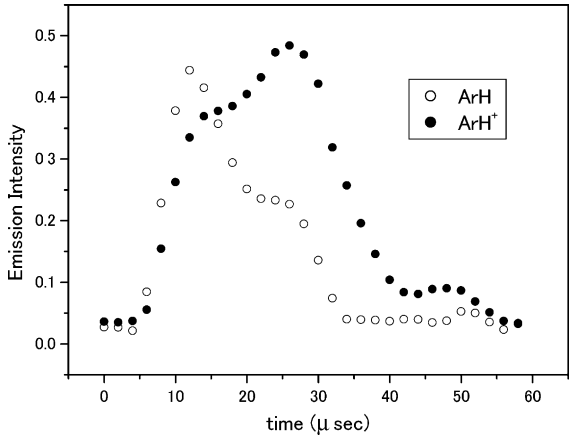


Fig. 5. Observed time profiles of emission intensities of $ArH^+v = 1$–0, R(7) [2725.5843 $cm^{-1}$] and ArH 5p–6s, R(6.5) [3700.774 $cm^{-1}$] lines. A discharge pulse was applied during 0–20 μs with a peak current of 0.8 A. The partial pressures are Ar 465 Pa and $H_2$ 53 Pa (high $H_2$ pressure condition). The abscissa values are relative intensities of the two lines.

We also observed the spectrum from a discharge (20 μs duration) with partial pressures of Ar 465(3.5) Pa(Torr) and $H_2$ 53(0.4) Pa(Torr) (high $H_2$ pressure condition) at a discharge current of 0.8 A. Similar pressure conditions gave the best signal-to-noise ratio for ArH in the DC discharge at a current of 0.45 A. Since relaxation processes by collision with hydrogen occurred much faster than in the low $H_2$ pressure discharge, we covered 60 μs at sampling interval of 2 μs. Fig. 5 shows the time profiles of the emission intensities of $ArH^+$ and ArH. The Ar line showed the same time profile as ArH. It is noted, however, that the time profile of ArH is different from that of $ArH^+$ and also that of ArH in a low $H_2$ pressure discharge.

## 4. Results and discussion

In the pulsed discharge studies by us, many processes are expected to occur simultaneously. Time-resolved FT spectroscopy offers the advantage of a systematic study of many chemical species simultaneously through high-resolution spectroscopy. A careful study of the observed spectra under both low and high $H_2$ pressure conditions, indicates that the $H_2$ pressure and metastable $Ar^*$ atoms play an important role in the present system. The $^3P_0$, $^3P_1$, and $^3P_2$ states of metastable $Ar^*$ have energies of 11.72, 11.62, and 11.55 eV, respectively, and the radiative lifetime is longer than a few ms. Therefore, under the present experimental conditions the species can survive even during the 'discharge-off' period, if the collisional de-excitation process is not effective. Under low $H_2$ pressure condition, such a situation is realized, and the metastable $Ar^*$ that survive will excite other $Ar^*$ atoms leading to emission which is responsible for the second peak in Fig. 4. The dissociative recombination reaction of $ArH^+$ and electron may also contribute to the second peak of Ar emission, where a dominant formation process of $ArH^+$ ion is proton transfer reaction during discharge, $H_2^+ + Ar \rightarrow ArH^+ + H$.

In Fig. 4, the peak of ArH was observed simultaneously with the second Ar emission peak. This means that the excited Ar atoms may be responsible for the ArH production. Lipton [11] used a Penning excitation source for XeH, where the Xe atom in the metastable state was shown to play an important role in the production of the rare-gas hydride. A similar mechanism may be at work in the present experiment. Since the ArH upper state $^2\Pi(5p)$ has an energy of 11.96 eV above the separate atom limit Ar + H, the energy of the metastable $Ar^*$ is not enough for the reaction $Ar^* + H_2 \rightarrow ArH + H$, to occur since the binding energy of $H_2$ is 4.74 eV. A three body reaction $Ar^* + H + M \rightarrow ArH + M$ may be responsible for the production of ArH. In the low $H_2$ pressure condition, the decay of the signals after the second maxima could be fitted to an exponential function with decay times of $23.0 \pm 1.7$ μs and $17.8 \pm 1.7$ μs for Ar and ArH, respectively. The ArH radical is an excimer, and the $^2\Pi(5p)$ state is strongly coupled with the repulsive ground state. The lifetime is predicted to be 42 ns by theoretical calculations of Theodorakopoulos and Petsalakis [12], where the radiative transition probability to the state $^2\Sigma^+(6s)$ observed is expected to be 10% of that to the ground state. Therefore the observed decay of ArH may not be genuine decay, but could be governed by the production process.

In afterglow plasma, the electron density becomes lower. On the other hand, metastable atoms can exist and may contribute in the production of new electronic states. Thus the ArH spectral lines were observed with better signal-to-noise ratio in the afterglow plasma of at low $H_2$ pressures as shown in Fig. 4, compared with the high $H_2$ pressure conditions shown in Fig. 5. This afterglow is electrically quiet plasma in which other fragile molecules may survive. We also detected many spectral lines in the 2800 $cm^{-1}$ region from the discharge under low $H_2$ pressure conditions, which are not clearly observed in a DC discharge. The time profile was similar to that of the ArH radical. The identification and analysis of these lines are in progress and will be published later.

## Acknowledgements

We are grateful to R. D'Cunha for a critical reading of the manuscript. The present study is

partially supported by a Grant-in-Aid by the Ministry of Education, Culture, Sports, Science and Technology of Japan (Grant No. 13440181).

## References

[1] G. Durry, G. Guelachvili, J. Mol. Spectrosc. 168 (1994) 82.
[2] N. Picqué, G. Guelachvili, Appl. Opt. 38 (1999) 1224.
[3] N. Picqué, G. Guelachvili, in: K. Itoh, M. Tasumi (Eds.), Fourier Transform Spectroscopy: Twelfth International Conference, Waseda University Press, Tokyo, 1999, p. 223.
[4] L. Letendre, D.-K. Liu, C.D. Pibel, J.B. Halpern, H.-L. Dai, in: K. Itoh, M. Tasumi (Eds.), Fourier Transform Spectroscopy: Twelfth International Conference, Waseda University Press, Tokyo, 1999, p. 115.
[5] R.E. Murphy, F.H. Cook, H. Sakai, J. Opt. Soc. Am. 65 (1975) 600.
[6] P.A. Berg, J.J. Sloan, Rev. Sci. Instrum. 64 (1993) 2508.
[7] T. Nakanaga, F. Ito, H. Takeo, Chem. Phys. Lett. 206 (1993) 73.
[8] H. Weidner, R.E. Peale, Appl. Spectrosc. 51 (1997) 1106.
[9] H. Weidner, R.E. Peale, Appl. Spectrosc. 52 (1997) 587.
[10] I. Dabrowski, D.W. Tokaryk, M. Vervloet, J.K.G. Watson, J. Chem. Phys. 104 (1996) 8245.
[11] R.H. Lipton, Chem. Phys. Lett. 129 (1986) 82.
[12] G. Theodorakopoulos, I.D. Petsalakis, J. Chem. Phys. 101 (1994) 194.